Polarization-based Inverse Rendering from Single View

Daisuke Miyazaki   Robby T. Tan

Kenji Hara   Katsushi Ikeuchi

Institute of Industrial Science
The University of Tokyo
4-6-1 Komaba, Meguro-ku, Tokyo
153-8505, Japan

e-mail: {miyazaki,robby,hara,ki}@cvl.iis.u-tokyo.ac.jp
http://www.cvl.iis.u-tokyo.ac.jp/

Abstract

This paper presents a method to estimate the geometrical, photometrical, and environmental information of a single-viewed object in one integrated framework. This three types of information is important to render a photorealistic image of a real object. In general, photometrical information represents the texture and the surface roughness of an object, while geometrical and environmental information represent the 3D shape of an object and the illumination distribution, respectively. We estimate the 3D shape, texture, and surface roughness of an object and the direction of the light sources from images with fixed view and illumination position. Specifically, the 3D shape is estimated by computing the surface normal from polarization data; the texture of the object is calculated from the diffuse only reflection component, after separating the reflection components based on colors; the illumination directions are determined from the position of the intensity peak in the specular reflection component; finally, the surface roughness of the object are computed by using the estimated illumination distribution. To evaluate the effectiveness of our estimation, we re-render synthetic images of objects using estimated information.

1 Introduction

To render a photorealistic image of a real object, we have to obtain the information of object's physical information. Three major types of information is usually used: geometrical, photometrical, and environmental information. The photometrical information provides the surface reflectance parameters (texture and surface roughness) of an object, while the geometrical and environmental information provides the shape of an object and the illumination distribution, respectively.

Many methods have been proposed to estimate each of the three types of information. Shape-from-X methods deal with the geometrical information estimation. Examples of these methods are shape-from-shading, visual hull, stereo, photometric stereo, polarization analysis, motion analysis, laser range finding, pattern light projecting, and so on. Generally, there are two classes of methods to estimate photometrical and environmental information: IBR (image-based rendering) and MBR (model-based rendering) methods. The IBR requires less information of

the shape of the object than the MBR, while the MBR requires less information of the image of the object than the IBR. The environmental information can be either obtained using several images taken from a number of viewpoints, or using a single view by utilizing a metal sphere or fisheye-lens camera.

Rendering this three types of information under less constraints are called inverse rendering. Tominaga et.al. [1] estimated shape, texture, and surface roughness. Zheng et.al. [2] and Nayar et.al. [3] estimated shape, texture, and illumination distribution. Sato et.al. [4], Ramamoorthi et.al. [5], Nishino et.al. [6], and Hara et.al. [7] estimated texture, surface roughness, and illumination distribution.

In this paper, we propose a method to obtain shape, texture, surface roughness, and illumination distribution from a single view at the same time in one integrated framework. The 3D shape is obtained by computing the surface normal from polarization data. The texture of the object is calculated from the diffuse only reflection component, after separating the reflection components of the images based on colors. The illumination directions are determined from the position of the intensity peak in the specular component. Finally, the surface roughness of the object is computed by using the estimated illumination distribution.

This paper is organized as follows: Section 2 shows a method to obtaining the surface shape of the object. Section 3 shows the method to estimate the texture, surface roughness, and illumination direction. Section 4 shows the measurement results and section 5 concludes this paper.

2   Modeling geometrical information

Shape of the object is computed from images taken by a polarizer-mounted camera. Before analyzing the polarization state of the input images, we apply a method described in section 2.1 to separate the reflection components. We analyze the polarization state of the diffuse only reflection component. Section 2.2 gives an introduction to the polarization phenomena. Section 2.3 and 2.4 describe the method to compute the surface normal of the object by analyzing the polarization data. At the end of this section, surface height is estimated by using a relaxation method [8,9].

2.1   Separating diffuse and specular components

Most inhomogeneous surfaces follow the dichromatic reflection model. According to this model, the intensity of the light reflected from an object surface is a linear combination of the diffuse and the specular reflection components [10](Figure 1). Before applying our method, we need to separate the input image into two component images, namely, specular component image and diffuse component image.

Many methods are proposed to separate the image into each components based on the color analysis [11–14]. In our method, Tan's method [15] is used for its robustness. This method requires illumination chromaticity normalization, so that the illumination chromaticity needs to be known beforehand; we can use white reference or color constancy algorithm to obtain the illumination chromaticity [16]. The normalization is done simply by dividing the image intensity using known illumination chromaticity: $\tilde{\mathbf{I}} = [I_R/i_r \ \ I_G/i_g \ \ I_B/i_b]^T$, where $\mathbf{I} = [I_R \ \ I_G \ \ I_B]^T$ is the image intensity in each color channel, and $\mathbf{i} = [i_r \ \ i_g \ \ i_b]^T$ is the illumination chromaticity.
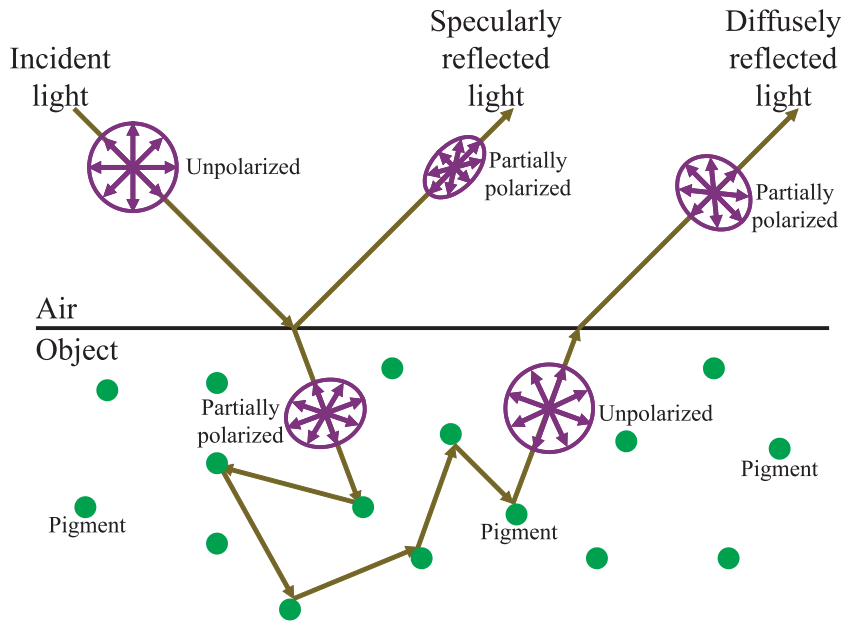
Figure 1: Specular and diffuse reflection.

In this paper, we assume that all light sources have the same color throughout the surface.

2.2   Polarization

Many shape-from-X techniques are proposed to estimate the surface shape from a single view. One of these methods is shape-from-polarization method [17–23]. This method estimates the surface normal of an object surface illuminated by incandescent lamp. Shape-from-polarization can estimate the surface normal of the object without knowing any illumination information.

We analyze the polarization phenomena of diffuse reflection component as follows: If one illuminates the object by unpolarized light, the light will branch off into two types of light: specular light and diffuse light [10](Figure 1).Specular light reflects at the interface of the air and the object, and go back into the air immediately. On the other hand, diffuse light penetrates inside the object, scatters randomly inside the object by reflecting at pigments, and goes back into the air. Both types of light will be partially polarized, however, diffuse light will become depolarized when scattering randomly inside the object, and such diffuse light will again become partially polarized when it emits out from the object to the air [19, 21]. The polarization state of diffuse light depends on the surface normal of the object, thus, by analyzing the polarization state of diffuse light, we can obtain the information about the shape of the object.

By observing the light by a linear polarizer mounted camera, we can obtain the polarization state of the light [17](Figure 2). Observed intensity will vary when the polarizer is rotated. This intensity difference forms a sinusoidal curve with respect to the angle of the rotation of the polarizer (Figure 3). We denote the maximum intensity of such sinusoidal curve as $I_{\max}$ and the minumum one as $I_{\min}$.

Surface normal can be represented as polar coordinate system (θ, ϕ) where θ is zenith angle and ϕ is azimuth angle($0° \leq \theta < 90°$, $0° \leq \phi < 360°$). Zenith angle is the angle between the
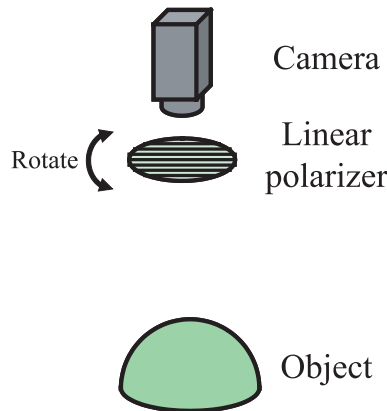
Figure 2: Acquisition system.

viewing direction and the surface normal, and azimuth angle is the orientation of the plane consisted of viewing direction and the surface normal. Zenith angle can be determined by DOP(degree of polarization), which the detail is described in section 2.3. The angle of the polarizer where we observe $I_{\max}$ will be the azimuth angle. Since the linear polarizer has a cycle of $180°$, we obtain two azimuth angles in the domain $0° \leq \phi < 360°$. One of those angles will equal to the true azimuth angle of the surface normal whereas the other faces the opposite direction. The procedure to resolve this ϕ-ambiguity is described in section 2.4.

2.3   Determining zenith angle

Figure 4 represents the emission of the diffuse light. We discuss the light emitted from inside the object. When the unpolarized incident light inside the object penetrates into the interface surface and transmits outside the object, such transmitted light becomes partially polarized. We express the angle between the incident light and the opposite direction from surface normal as θ_1, and the angle between the transmitted light and the surface normal as θ_2. We call the plane consisted of the incident light and transmitted light an incident plane.

Light oscillates orthogonally to the direction of the traveling light. The ratio of the incident intensity to the transmitted intensity is called the intensity transmissivity. We denote the intensity transmissivity of parallel component to the incident plane as T_p and that of perpendicular component as T_s. The intensity transmissivity of p-component T_p and that of s-component T_s are [17]:

$$T_p = \frac{n_2 \cos \theta_2}{n_1 \cos \theta_1} t_p^2 \tag{1}$$

$$T_s = \frac{n_2 \cos \theta_2}{n_1 \cos \theta_1} t_s^2 \tag{2}$$

where n_1 and n_2 are the refractive index of the object and the air respectively. t_p and t_s are the amplitude transmissivity of p-component and s-component, and expressed as:

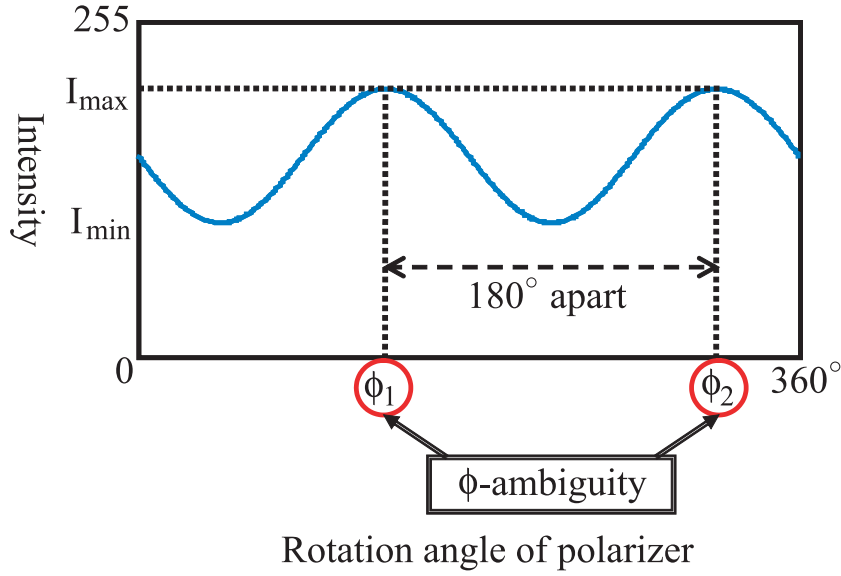$$t_p = \frac{2 \sin \theta_2 \cos \theta_1}{\sin(\theta_1 + \theta_2) \cos(\theta_1 - \theta_2)} \tag{3}$$

Figure 3: Relation between the rotation angle of polarizer and the observed intensity.

$$t_s = \frac{2\sin\theta_2\cos\theta_1}{\sin(\theta_1+\theta_2)} \quad . \tag{4}$$

By substituting equation (??) and (4), and Snell's law, $n_1\sin\theta_1 = n_2\sin\theta_2$, into equation (1) and (2) we obtain:

$$T_p = \frac{4\cos\theta\sqrt{n^2-\sin^2\theta}}{1+n^2-(n^2+1/n^2)\sin^2\theta+2\cos\theta\sqrt{n^2-\sin^2\theta}} \tag{5}$$

$$T_s = \frac{4\cos\theta\sqrt{n^2-\sin^2\theta}}{1+n^2-2\sin^2\theta+2\cos\theta\sqrt{n^2-\sin^2\theta}} \tag{6}$$

where n is the refractive index of the object to that of the air ($n = n_1/n_2$), and $\theta = \theta_2$. The graph of T_p and T_s are shown in Figure 5. From equation (5) and (6), T_p is always greater than T_s. Thus, $I_{\max}$ and $I_{\min}$ are expressed by using the total intensity of the transmitted light I as:

$$I_{\max} = \frac{T_p}{T_p+T_s}I, \quad I_{\min} = \frac{T_s}{T_p+T_s}I \quad . \tag{7}$$

DOP(degree of polarization) represents how much the light has been polarized. DOP is 1 for perfectly polarized light, 0 for unpolarized light, and it varies between 0 to 1. The definition of DOP is:

$$\rho = \frac{I_{\max}-I_{\min}}{I_{\max}+I_{\min}} \tag{8}$$

Substituting equation (5) and (6) into equation (8), we obtain:

$$\rho = \frac{(n-1/n)^2\sin^2\theta}{2+2n^2-(n+1/n)^2\sin^2\theta+4\cos\theta\sqrt{n^2-\sin^2\theta}} \tag{9}$$
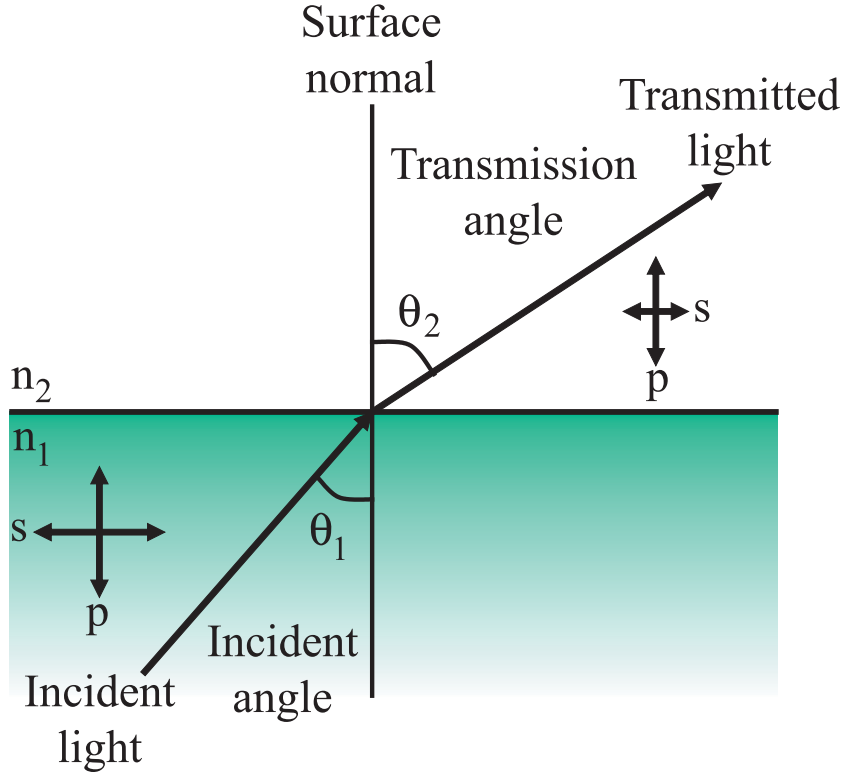
Figure 4: Diffuse light emitted from inside the object.

This ρ is the DOP of diffuse light, and θ is the zenith angle. Figure 6 represents this function.

Equation (9) depends on the refractive index. We assume that the refractive index of an object is same for all parts of an object. Many objects we want to measure have a refractive index of 1.5 to 1.7. Thus, we set the refractive index as 1.7. If the refractive index is less than 1.7, then, DOP will be lowered. We have to estimate the attenuation of DOP. In addition, equation (9) is derived by assuming the surface as an optically smooth surface. Rough surface causes depolarization and lowers the obtained DOP. As a result, we modify the obtained data and calculate the DOP as follows:

$$\rho = \frac{I_{\max} - I_{\min}}{I_{\max} + I_{\min} - u} \tag{10}$$

where $u(\geq 0)$ is the modification factor. Equation (10) indicates that we subtract the intensity of unpolarized light $u/2$ from the input intensity, $I_{\max}$ and $I_{\min}$, each. This modification raises the value of DOP.

Equation (9) have an extremum at $\theta = 90°$. We assume that the object is a closed, C^∞ surface. Thus, we always observe a point whose zenith angle θ equals to $90°$, and the zenith angle θ of occluding boundary always equals to $90°$. First, we choose m points of occluding boundary and sort by ascent order with respect of DOP. Then, for certain i and j where
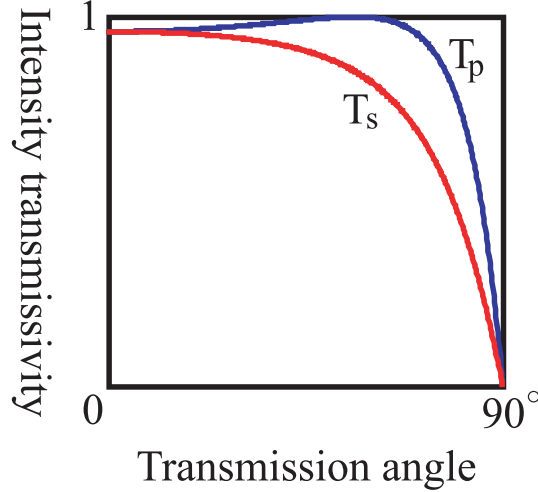
Figure 5: Intensity transmissivity($n = 1.5$).

$1 \leq i \leq j \leq m$, we calculated the following equation derived from equation (10):

$$u = \frac{\displaystyle\sum_{k=i}^{j} \left[I^{(k)}_{\max} + I^{(k)}_{\min} - \frac{I^{(k)}_{\max} - I^{(k)}_{\min}}{\rho(90^\circ)} \right]}{\displaystyle\sum_{k=i}^{j}} \quad . \tag{11}$$

If there are no noise in input data, we can set i and j to m, however, we set those values for certain values.

2.4   Determining azimuth angle

Since the linear polarizer has a cycle of 180°, we obtain two azimuth angles in the domain $0^\circ \leq \phi < 360^\circ$. One of those angles equals to the true azimuth angle of the surface normal where the other heads the opposite direction. We assume the object as a closed C^∞ object, thus, we can determine the surface normal of the occluding boundary. We also assume the object has no perfect concave area, the area which is always concave when observed from any direction. Those concave part causes strong interreflection and it perturbs the measurement of polarization state and the estimation of light sources, thus, we assume there is no interreflection. As a result, we can determine the azimuth angle by determining the azimuth angle from the occluding boundary towards the inside area of the object.

  Equation we have to minimize is:

$$\iint (\nabla \Phi)^2 + \hat{\lambda} (\Phi - \Phi_0)^2 \; dx \, dy \tag{12}$$

where $\hat{\lambda}$ is a positive constant, Φ is the azimuth angle, and Φ_0 is the value depending on the input azimuth angle. Here, azimuth angle is expressed as 2-dimensional vector:

$$\Phi = \begin{pmatrix} \cos \phi \\ \sin \phi \end{pmatrix} \tag{13}$$

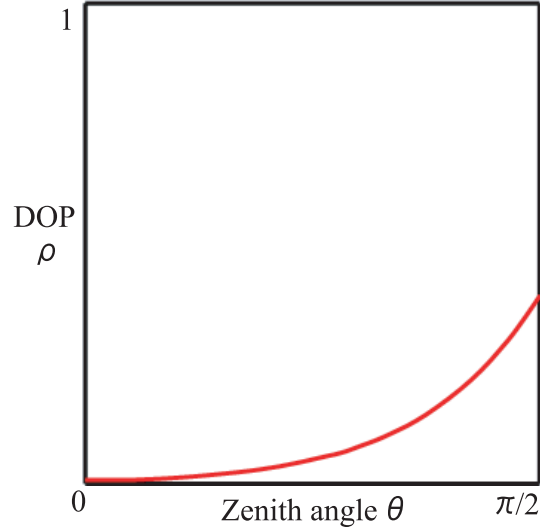Figure 6: DOP(degree of polarization) of diffuse light $(n = 1.7)$

The solution to the equation (12) is:

$$\Phi^{(i+1)}(x,y) = \frac{\bar{\Phi}^{(i)}(x,y) + \lambda \Phi_0^{(i)}(x,y)}{1 + \lambda} \tag{14}$$

where λ is a positive constant, $\Phi^{(i+1)}(x,y)$ is the azimuth angle of $(i+1)$th iteration and $\bar{\Phi}^{(i)}(x,y)$ is the average azimuth angle of the 4-neighborhood of (i)th iteration. We calculate $\Phi_0^{(i)}(x,y)$ as follows:

1. If $\Phi^{(i)}$ is not yet determined, then $\Phi_0^{(i)} = 0$.

2. Else: Denote the two possible azimuth angles as Φ_1 and Φ_2.

    (a) If $(\Phi^{(i)} - \Phi_1)^2 \leq (\Phi^{(i)} - \Phi_2)^2$ then $\Phi_0^{(i)} = \Phi_1$.
    (b) Else $\Phi_0^{(i)} = \Phi_2$.

We set the initial value for the iteration as $\Phi = 0$ except for occluding boundary. We calculate the surface normal at occluding boundary as a vector facing outside of the object area, and set Φ as such value at occluding boundary.

3   Modeling photometrical and environmental informa-tion

Section 3.1 shows the method to estimate the direction of illumination. Section 3.2 shows the method to estimate texture and surface roughness.
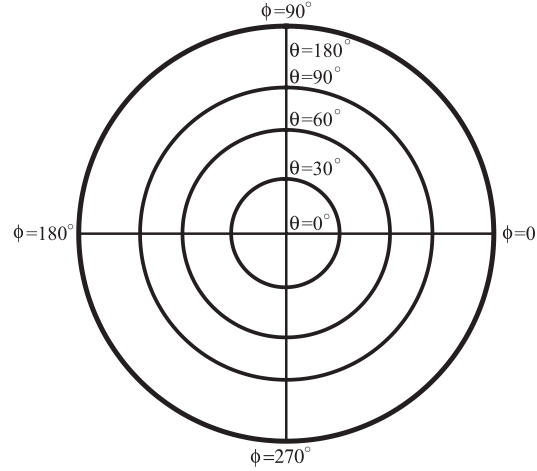
Figure 7: Illumination map which represents the illumination distribution in polar coordinate system (θ, ϕ).

3.1 Estimating illumination direction

The direction of the light source can be represented as a polar coordinate system; we do not estimate the distance between the light source and the object, and we assume that the light sources are sufficiently far from the object.

We denote the representation of illumination distribution as an illumination map(Figure 7). First, we project the specular intensity onto an illumination map in a perfect mirror direction: For each point in the object image, we know the specular intensity I_s and the surface normal (θ, ϕ), thus, we set I_s at $(2\theta, \phi)$ on the illumination map. Next, by thresholding the illumination map and eliminating the noise, we will obtain some regions on the illumination map whose number equals to the number of light sources. Here, we assume that the light sources are far from each other. Finally, we determine the direction of light sources from the position of the peak intensity in each regions.

3.2 Estimating reflection parameters

In this paper, we use simplified and discretized Torrance-Sparrow model [10] for the reflection model:

$$I = I_d + I_s \tag{15}$$

$$I_d = K_d \left(\sum_{l=1}^{L} \cos \theta_i \right) \Delta\omega \tag{16}$$

$$I_s = \frac{K_s}{\cos \theta_r} \left(\sum_{l=1}^{L} \exp \left(-\frac{\alpha^2}{2\sigma^2} \right) \right) \Delta\omega \tag{17}$$

where I is the observed intensity, I_d is the diffuse reflection intensity, I_s is the specular reflection intensity, K_d is the diffuse reflection scale, θ_i is the angle between the incident light and the surface normal, K_s is the specular reflection scale, θ_r is the angle between the surface normal
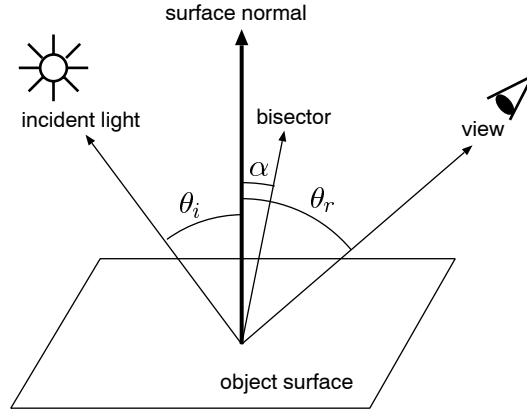
Figure 8: Geometrical location of surface normal, illumination direction, and viewing direction

and the viewing direction, α is the angle between the surface normal and the bisector of incident light direction and the viewing direction, σ is the surface roughness paramter, $l = \{1, ..., L\}$ is a set of light sources, and $\Delta\omega$ is the size of a light source(Figure 8).

Estimating both illumination intensity and reflection scale(K_d and K_s) is an ill-posed problem, thus, we only estimate the reflection scale. We assume that the Fresnel coefficient and the geometrical attenuation factor are constant in this section. In this paper, we use RGB color camera, thus, I, I_d, I_s, K_d, and K_s are 3-dimensional vectors.

We obtain I from the camera, I_d and I_s by separating reflection components, θ_i, θ_r, and α by surface normal and illumination, and we give the value of $\Delta\omega$. We estimate L by the procedure described in section 3.1. We have to estimate the diffuse reflectance K_d, the specular reflectance K_s, and surface roughness σ.

Diffuse reflectance is sometimes called a texture. From surface normal and illumination distribution, we can calculate the diffuse reflectance K_d from equation (16).

We assume that all of surface points have the same K_s and σ. K_s and σ can be estimated by non-linear least square method.

4   Measurement results

Figure 13(a) shows a real image of a green hemisphere we will measure. By the color-based separation, we separated the input image into specular and diffuse component images. From the polarizer-mounted camera, we obtained the DOP data and ϕ data from the diffuse component image(Figure 9). Then, we calculated the surface normal of the object and integrated them into the height of the object(Figure 10).

We projected the specular intensity into the illumination map with perfect mirror direction with respect to the surface normal(Figure 11(a)). By thresholding the illumination map, some regions came in sight (Figure 11(b)). Note that we eliminated some noises by image processing technique. Then, we obtained that the number of light source is three, as regions' number is three. We determined the direction of the light source from the peak point in each region. Estimated light source direction is depicted in Figure 12(a). For comparison, the true illumi-
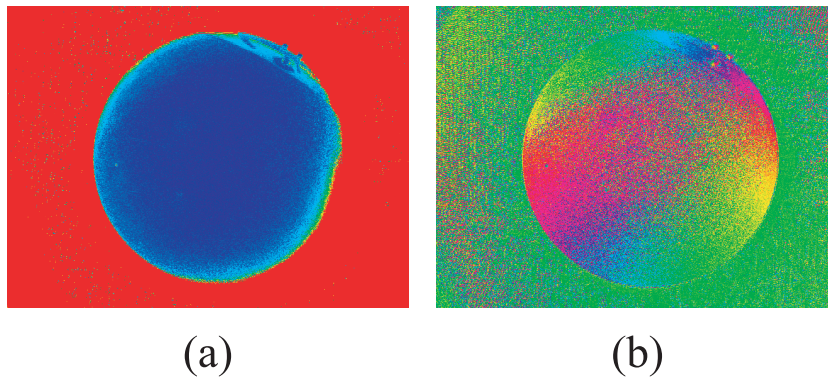
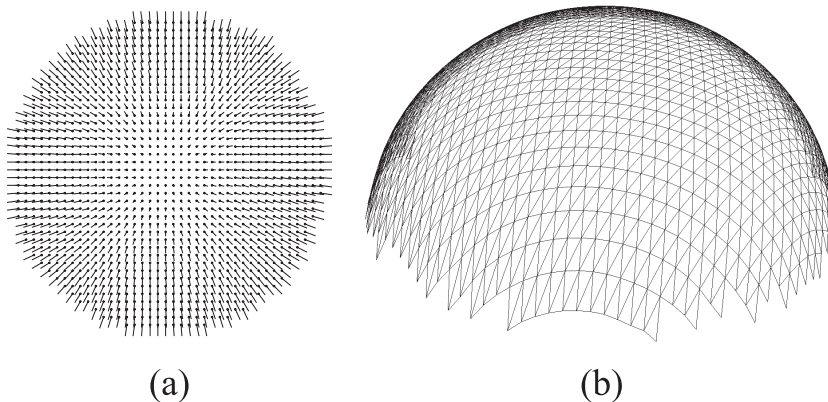Figure 9: Polarization data of hemisphere: (a) DOP image, (b) Phase angle image

Figure 10: Estimated shape of hemisphere: (a) Needle map, (b) Surface mesh

nation distribution is shown in Figure 12(b). Estimated texture K_d was (20000, 42000, 20000). For the measurement results described in this paper, we assumed that K_d is the same for all surface points. We estimated the reflection parameters iteratively from surface normal and illumination. Estimated surface roughness σ was 0.11, and estimated specular scale K_s was 24000. Note that we normalized the input images to make the illumination become white, thus, K_s is also white.

Rendered example is shown in Figure 13(b) and (c). For comparison, real image is shown in Figure 13(a). Figure 13(b) is rendered under the estimated parameters and illumination, which should be the same as Figure 13(a). Figure 13(c) is an another example which is rendered under the different object direction and the different illumination position.

Figure 15(a) shows an image of a yellow pear object. Estimated illumination is depicted in Figure 14(a) with the ground truth in Figure 14(b). The rendered image based on the estimated parameters is shown in Figure 15(b), another rendered image with different view and illumination is shown in Figure 15(c), and the surface mesh is shown in Figure 15(d). Surface roughness σ was estimated to be 0.16, K_s was 15000, and K_d was (34000, 20000, 7800).
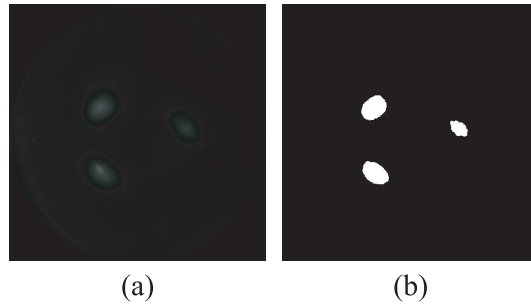
(a)   (b)

Figure 11: Illumination map of hemisphere: (a) Intensity projected onto illumination map in a perfect mirror direction, (b) Illumination candidate regions
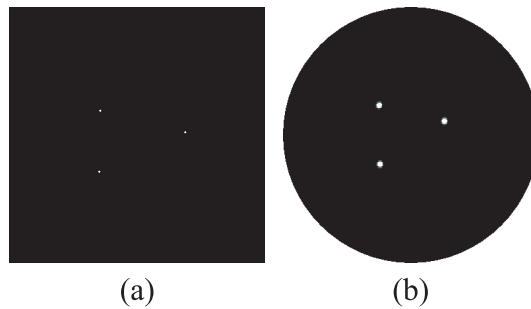

(a)   (b)

Figure 12: Illumination of hemisphere: (a) Estimated illumination, (b) True illumination

5   Conclusion

We proposed a method to estimate shape, texture, surface roughness, and illumination distribution from a single view in one integrated framework. Our method estimates the direction of multiple light sources, which does not require any special light sources such as laser beam nor structured pattern light. One of our main contributions is the improvement of the shape-from-polarization technique. We successfully obtained the shape of the object from a single view by analyzing the polarization effect of the light, and demonstrated the ability of our method to determine the shape of objects using real images. We also estimated the reflection parameters and illumination distribution to confirm that the estimated shape is enough precise to be applied to another process.

Our future work is to discuss the precision of our system, and improve the precision as high as possible. The goal is to develop a system to easily measure the whole indoor environment.

References

[1] S. Tominaga and N. Tanaka, "Estimating Reflection Parameters from a Single Color Image," *IEEE Computer Graphics and Applications*, pp. 58-66, 2000.

[2] Q. Zheng and R. Chellapa, "Estimation of Illuminant Direction, Albedo, and Shape from
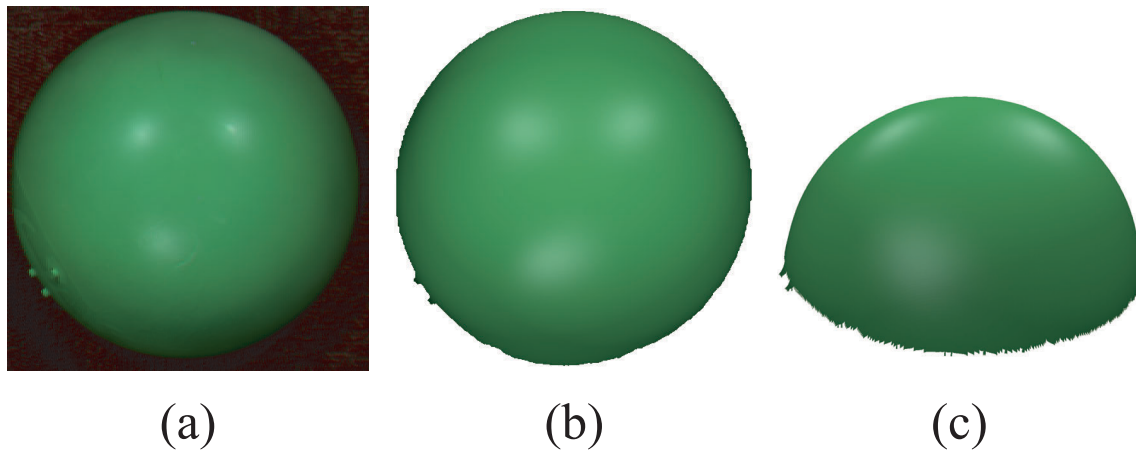
Figure 13: Result of hemisphere: (a) True image, (b) Synthesized image, (c) Rendered from a novel view under different illumination
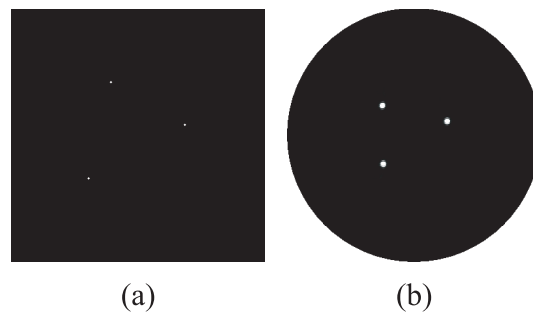

Figure 14: Illumination of pear: (a) Estimated illumination, (b) True illumination

Shading," *IEEE Transactions on Pattern Analysis and Machine Intelligence*, Vol. 13, No. 7, pp. 680-702, 1991.

[3] S. K. Nayar, X. S. Fang, and T. Boult, "Separation of Reflection Components Using Color and Polarization," *International Journal of Computer Vision*, 1996.

[4] I. Sato, Y. Sato, and K. Ikeuchi, "Illumination distribution from brightness in shadows: adaptive estimation of illumintion distribution with unknown reflectance properties in shadow regions," *ICCV 99*, pp. 875-882, 1999.

[5] R. Ramamoorthi and P. Hanrahan, "A signal processing framework for inverse rendering," *Proceedings of SIGGRAPH 2001*, pp. 379-387, 2001.

[6] K. Nishino, Z. Zhang, and K. Ikeuchi, "Determining Reflectance Parameters and Illumination Distribution from a Sparse Set of Images for View-dependent Image Synthesis," *Proc. of Eighth IEEE International Conference on Computer Vision*, pp. 599-606, 2001.

[7] K. Hara, K. Nishino, A. Nakazawa, and K. Ikeuchi, "Estimating Light Position and Surface
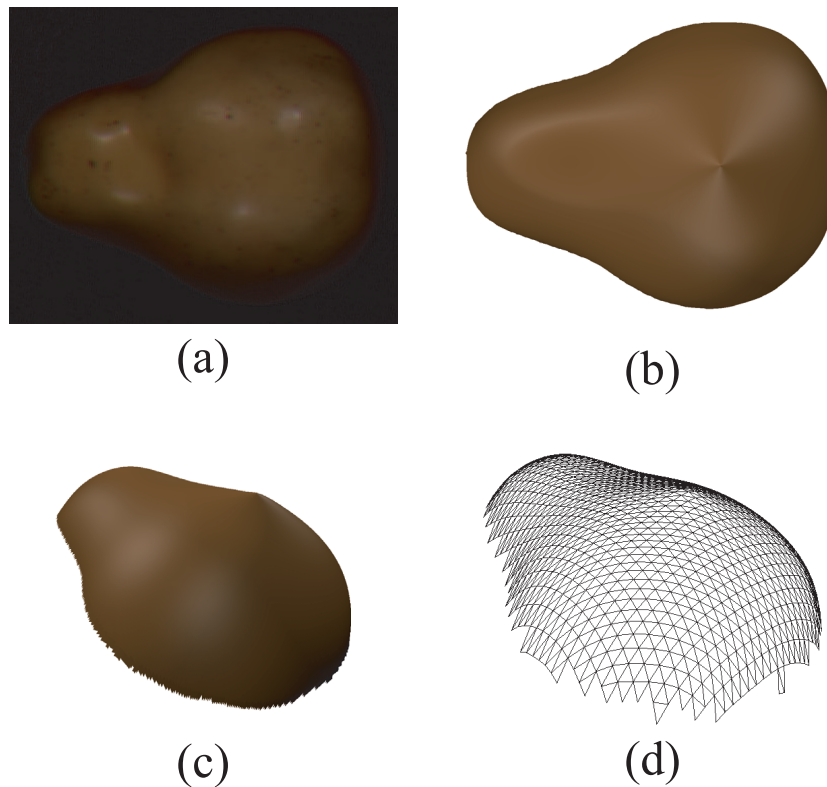
Figure 15: Result of pear: (a) True image, (b) Synthesized image, (c) Rendered from a novel view under different illumination, (d) Surface mesh

Reflectance from Specular Reflection under Perspective Projection," *Proceedings of IAPR Workshop on Machine Vision Applications*, pp. 566-571, 2002.

[8] B. K. P. Horn, *Robot vision*, MIT Press, 1986.

[9] K. Ikeuchi, "Reconstructing a depth map from intensity maps," *Proc. Intl. Conf. Pattern Recognition*, Montreal, Canada, pp. 736-738, 1984.08

[10] K. E. Torrance and E. M. Sparrow, "Theory for off-specular reflection from roughened surfaces," *J. Opt. Soc. Am.*, Vol. 57, No. 9, pp. 1105-1114, 1967.

[11] G. J. Klinker, S. A. Shafer, and T. Kanade, "The measurement of highlights in color images," *International Journal of Computer Vision*, pp. 2:7-32, 1990.

[12] S. W. Lee and R. Bajcsy, "Detection of specularity using color and multiple views," *Image and Vision Computing*, pp. 10:643-653, 1990.

[13] R. Bajscy, S. W. Lee, and A. Leonardis, "Detection of diffuse and specular interface reflections by color image segmentation," *International Journal of Computer Vision*, Vol. 17, No. 3, pp. 249-272, 1996.

[14] S. Lin and H. Y. Shum, "Separation of diffuse and specular reflection in color images," *Conference on Computer Vision and Pattern Recognition*, 2001.

[15] R. T. Tan, K. Nishino, and K. Ikeuchi, "Separating Diffuse and Specular Reflection Components based on Surface Color Ratio and Chromaticity," *Proceedings of IAPR Workshop on Machine Vision Applications*, pp. 14-19, 2002.

[16] R. T. Tan, K. Nishino, and K. Ikeuchi, "Illumination Chromaticity Estimation using Inverse-Intensity Chromaticity Space," to appear in *IEEE Conf. Computer Vision and Pattern Recognition*, Madison, Wisconsin, 2003.

[17] M. Born and E. Wolf, *Principles of optics*, Pergamon, 1959.

[18] K. Koshikawa, and Y. Shirai, "A model-based recognition of glossy objects using their polarimetrical properties," *Advanced Robotics*, Vol. 2, No. 2, pp. 137-147, 1987.

[19] L.B. Wolff, and T.E. Boult, "Constraining object features using a polarization reflectance model," *IEEE Trans. Pattern Analysis and Machine Intelligence*, Vol. 13, No. 7, pp. 635-657, 1991.07

[20] M. Saito, Y. Sato, K. Ikeuchi, and H. Kashiwagi, "Measurement of surface orientations of transparent objects by use of polarization in highlight," *J. Optical Society of America A*, Vol. 16, No. 9, pp. 2286-2293, 1999.09

[21] S. Rahmann, and N. Canterakis, "Reconstruction of specular surfaces using polarization imaging," *Proc. IEEE Conf. Computer Vision and Pattern Recognition*, Kauai Marriott, Hawaii, pp. I:149-155, 2001.12

[22] D. Miyazaki, M. Saito, Y. Sato, and K. Ikeuchi, "Determining surface orientations of transparent objects based on polarization degrees in visible and infrared wavelengths," *J. Optical Society of America A*, Vol. 19, No. 4, pp. 687-694, 2002.04

[23] Daisuke Miyazaki, Masataka Kagesawa, Katsushi Ikeuchi, "Determining Shapes of Transparent Objects from Two Polarization Images," *Proceedings of IAPR Workshop on Machine Vision Applications*, pp. 26-31, 2002.12